2012

Absolute cross sections for elastic electron scattering from methylformamide

J B. Maljkovic
University Of Belgrade

F Blanco
Universidad Complutense, Spain

G Garcia
University of Wollongong

B P. Marinkovic
University Of Belgrade

A R. Milosavljevic
University Of Belgrade

Publication Details

Maljkovic, J. B., Blanco, F., Garcia , G., Marinkovic, B. P. & Milosavljevic, A. R. (2012). Absolute cross sections for elastic electron scattering from methylformamide. Physical Review A: Atomic, Molecular and Optical Physics, 85 (4), 042723-1-042723-8.

Absolute cross sections for elastic electron scattering from methylformamide

J. B. Maljković,[1] F. Blanco,[2] G. García,[3,4] B. P. Marinković,[1] and A. R. Milosavljević[1,*]

[1]*Laboratory for Atomic Collision Processes, Institute of Physics, University of Belgrade, Pregrevica 118, 11080 Belgrade, Serbia*

[2]*Departamento de Física Atómica Molecular y Nuclear, Facultad de Ciencias Físicas, Universidad Complutense, Avenida Complutense s/n, E-28040 Madrid, Spain*

[3]*Instituto de Fisica Fundamental, Consejo Superior de Investigaciones Cientificas, Serrano 113-bis, 28006 Madrid, Spain*

[4]*Centre for Medical Radiation Physics, University of Wollongong, NSW 2522, Australia*

(Received 5 March 2012; published 30 April 2012)

Elastic electron scattering from gaseous methylformamide (*N*-methylformamide, C_2H_5NO) has been investigated. Absolute elastic differential cross sections (DCSs) were determined both experimentally and theoretically for the incident energies from 50 to 300 eV. The measurements were performed using a cross-beam technique, for scattering angles from 20° to 110°. Relative elastic DCSs were measured as a function of both the angle and the incident energy and the absolute DCSs were determined using the relative flow method. The calculations of electron interaction cross sections are based on a corrected form of the independent-atom method, known as the SCAR (screen corrected additivity rule) procedure and using an improved quasifree absorption model. Calculated integral cross sections have been presented, as well, both for methylformamide and formamide, in the energy range 10–1000 eV, and discussed. The results are compared with and discussed regarding existing data for other small molecules representing building blocks of large biomolecules.

DOI: 10.1103/PhysRevA.85.042723 PACS number(s): 34.80.Bm

I. INTRODUCTION

The formamide molecule and its derivates, such as *N*-methylformamide (NMF), C_2H_5NO, have been attracting considerable attention in recent years due to their importance as prebiotic compounds and the simplest models of the peptide linkage NH–C=O (Fig. 1). The very recent photoionization mass spectrometric studies of formamide and NMF [1] have been carried out mainly within exobiological context, since these species had been observed in the interstellar medium, in star-forming regions [2]. The aim of the later investigation was to access the viability of these species in various sites in space and a possible influence of VUV photon irradiation. Furthermore, it has been shown that low-energy (4–20 eV) electron irradiation of a binary mixture of ammonia and acetic acid prepared at 25 K on polycrystalline hydrogenated diamond film-induced formation of a unique chemical species, without the need of thermal activation [3]. Therefore, investigation of electron interaction with isolated prebiotic molecules may be of importance for exobiology research and electron-induced chemistry in the interstellar media, where the presence of free electrons is expected [4].

On the other hand, investigation of electron interaction with small biomolecules representing building blocks of large biosystems (RNA, DNA, proteins) has been mainly motivated in recent years by radiation damage research. It has been shown that secondary low-energy electrons can cause significant, energy-dependent single- and double-strand breaks in DNA [5,6]. Since the major part of the energy deposited by ionizing radiation in condensed matter is channeled into the production of abundant low-energy secondary electrons, spectroscopic data and absolute cross-section values for electron impact on biomacromolecules (DNA, proteins) and its constituents are needed in order to improve our understanding of the chain of reactions leading to radiation damage. It should be noted that high-energy particles, such as energetic ions that are of high interest in cancer therapy [7,8], may induce quite a broad energy spectrum of secondary electrons tailing to hundreds of eVs [9]. With this respect, our previous work includes measurements of absolute differential cross sections for electron scattering from several different molecules representing backbone sugar and nucleobasis subunits of DNA [10–12]. The peptide bond is a covalent linkage between amino acids, forming the primary structure of proteins [3]. Therefore, NMF has been considered as a model compound to investigate electron collisions from protein constituents. Kawashima and coauthors [13] have recently carried out a detailed investigation on the dynamical structure of peptide molecules. NMF has a planar structure, with two different isomers depending on the position of the CH_3 group (*trans*-NMF is presented in Fig. 1). Finally, it should be noted that NMF represents an important molecule in other aspects, as well, besides radiation damage and exobiological research, such as antitumor activities [14].

According to our knowledge, there are no published absolute differential cross sections (DCSs) for elastic electron scattering from NMF. However, the DCSs for elastic electron scattering from formamide, which is the smallest molecule that contains a peptide bond, have been reported the most recently by our group, for a few selected incident energies [15]. Also, Bettega [16] has reported results for integral and momentum transfer cross sections for elastic scattering of low-energy electrons (1–12 eV) from formamide, which have been calculated by employing the Schwinger multichannel method. In the present study, we report a set of absolute DCSs for elastic electron-NMF scattering in the energy range from 50 to 300 eV. The measured DCSs are in very good agreement with the calculations, both on the absolute scale and considering the DCS shape. Furthermore, calculated integral cross sections (ICSs) have been presented in the energy range from 10 to 1000 eV, both for NMF and formamide.

*vraz@ipb.ac.rs

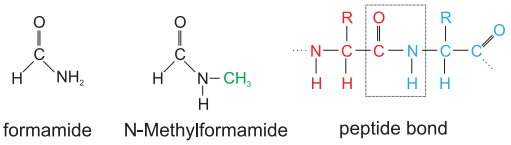

FIG. 1. (Color online) Schematic drawing of formamide (CH_3NO), *trans-N*-methylformamide (C_2H_5NO) and peptide bond linking two amino acids.

II. EXPERIMENT

Our apparatus and experimental procedures have been described in detail in previous papers [11,17] and only a brief description will be given here. The experimental setup consists of an electron gun, a double cylindrical mirror energy analyzer (DCMA), and a channel electron multiplier as detector. All components are enclosed in a double μ-metal shielded vacuum chamber. The base pressure of about 4×10^{-7} mbar was obtained by a turbomolecular pump, while the working pressure was usually kept in the range $(2–5) \times 10^{-6}$ mbar. An electron gun, with a hairpin electron source, produces a nonmonochromated electron beam that is crossed perpendicularly by a molecular beam, obtained by a non-magnetic stainless steel needle. The scattered electrons are focused by a four-element cylindrical electrostatic lens into the DCMA, followed by a three-element lens to further focus the transmitted electron beam into the channel multiplier. In the present work, the electron gun can be rotated around the needle in the angular range from about -40° to 110°. The uncertainty of the incident energy scale was determined to be less than ± 0.4 eV. The best energy resolution is limited by a thermal spread of primary electrons to about 0.5 eV. The angular resolution is better than $\pm 2^\circ$ [17].

The anhydrous NMF was purchased from Aldrich with declared purity better than 99% and was used after several freeze-pump-thaw cycles under vacuum, which were performed before each set of measurements. NMF is a liquid at room temperature and was introduced into the scattering region from a glass container via a gas line system. The whole gas-handling system (sample container, pipes, needle) was heated to provide stable experimental conditions and to improve the signal.

In the present work DCSs for elastic electron scattering from NMF have been measured at selected incident electron energies, from 50 to 300 eV (in 50 eV steps), and at scattering angles from 20° to 110° (in 10° steps). At a given electron energy, the relative cross section has been derived as a function of the scattering angle by measuring the elastic scattering intensity at the maximum of the elastic peak. The background contributions of the elastic electron intensities, which were around 5% at higher energies and up to 15% at lower, have been measured by directing the molecular beam through the side leak and were subtracted from the measured electron yields. The calibration of both angular scale and true zero angular position, as well as the reliability of DCS shapes, have been tested according to DCSs for elastic electron-Ar scattering. The latter were obtained under the same experimental conditions, and showed very good agreement with previous results [18].

In the present studies we have also measured energy dependence of the DCSs over limited electron energy ranges, 50–300 eV (in 50–eV steps), for a fixed scattering angle of 40°. In this case, the voltages of both the focusing part of the electron gun and the four-element entrance analyzer lens were adjusted as a function of the applied incident energy in order to obtain constant incident electron beam and transmission function [17]. The procedure was checked according to DCSs for Ar, measured as a function of incident energy and compared with known results [18].

The relative-angle-dependent cross sections were further normalized to the absolute points obtained at several scattering angles (40°, 80°, or 90°) using the relative flow technique [19–21] and Ar as a reference gas, whose DCSs are known from both theoretical [22] and experimental [18,23] studies. In this method signal intensities of scattered electrons for the target and the referent gas are compared, at fixed scattering angle (θ) and electron energy (E), under the same experimental conditions. To provide the same experimental conditions one should ensure the same beam profiles for the target and referent gas, leaving the focusing properties of the electron gun and the detection system unchanged. It has been shown [19,21] that the profile of the gas beam depends primarily on the gas's mean free path over a range of pressures behind the gas tube, and if any two targets are made to separately flow through the same tube with the same mean free path, their profiles should remain identical. According to gas kinetic theory the mean free path is inversely proportional to the squared gas kinetic diameter (R); therefore it is widely used to keep the pressure ratio for the investigating target and the referent gas as $P_x : P_{\mathrm{ref}} = R_{\mathrm{ref}}^2 : R_x^2$ in order to obtain the same beam profiles. If these conditions are achieved, intensities of scattered electrons are converted into absolute differential cross sections (DCS) via the formula

$$\mathrm{DCS}_x\,(E,\theta) = \mathrm{DCS}_{\mathrm{ref}}\,(E,\theta)\,\frac{N_x F_{\mathrm{ref}}}{N_{\mathrm{ref}} F_x}\sqrt{\frac{M_{\mathrm{ref}}}{M_x}}, \qquad (1)$$

where N is the scattered electron intensity, F is the relative flow rate, and M is the molecular weight. The subindices x and *ref* refer to the gas under investigation and the referent gas, respectively. It should be noted that the described procedure requires the gas kinetic diameters to be known, which is not always the case, especially for liquid biotargets, as used in the present experiment. However, a group of authors [21,24] have recently developed an alternative version of the relative flow method using an aperture gas collimating source, to replace the conventional tube. For such a source, until the mean free path is greater than thickness of the aperture, angular distribution of the target beam is constant, so the authors were able to apply the relative flow method without the restriction imposed by the requirement that the pressures behind the source be in the ratio with the gas kinetic molecular diameters squared. Therefore, the importance of gas kinetic diameters depends on the particular experimental setup. In the present measurements, the pressure of NMF behind the tube forming the molecular beam was maintained below 0.2 mbar. The ratio of the pressures behind the tube for NMF to that of Ar was adjusted to be 1.4, the same as used for formamide, according to available gas kinetic diameters of similar molecules [15]. It

should be also noted that during the measurements it has been proved by varying the ratio of the Ar and NMF pressures that absolute values of the cross sections do not depend crucially on the pressure ratio to within uncertainties in the measured cross sections. Actually, similarly as reported previously for formamide [15], the experimental challenge was to obtain stable conditions.

The schematic drawing of the present relative flow experimental setup has been given in our most recent publication [15], while the measurement procedure has been also described in more detail previously [11]. Briefly, for each experimental point (fixed energy and angle) we have measured the signal intensity for NMF and Ar, as well as background (containing both NMF and Ar) contributions (usually about 20%, which were subtracted from the signal) and the relative flow rate (quantity F in formula 1). Both the vapors from the sample container and the referent gas (Ar) can be introduced into the vacuum chamber through the capillary or through the side leak. The relative flow rate has been determined by closing the outlet to the chamber, admitting vapors into a closed volume, and measuring the pressure increase over time. Since the closed volume is constant, we can assume that the pressure rise over time (measured by an MKS Baratron) is proportional to the outflow of vapors from the sample container. Here, it should be noted that for vapors, unlike for gaseous targets (e.g., Ar), effects such as adsorption on surfaces may significantly affect the flow rate determination and consequently the absolute differential cross sections, which have been investigated in detail recently by Homem *et al*. [25]. However, the influence of these effects was strongly reduced in the present case because the whole system (sample, pipes, valves, and needle) was heated, as also pointed out in [25]. Indeed, we have compared flow rates of NMF vapors measured at room temperature and when the gas line was maintained at 50°–60°, under the same pressures behind the needle, the results showed a non-negligible difference.

The final set of absolute DCSs is consistent with all three types of independently experimentally obtained results: relative DCSs as a function of the scattering angle at fixed incident energy, relative DCSs as a function of the incident energy at fixed scattering angle, and absolute (relative flow) measurements crossed with calculations. Comparison of all these independent sets of results allows checking of the experimental procedure and possible inconsistencies of reference cross sections.

The errors for the relative DCSs measured as a function of the scattering angle include statistical errors (0.2%–5%) according to Poisson's distribution and short-term stability errors (0.3%–7.5%) according to discrepancy of repeated measurements at the same incident energy and scattering angle. The errors for the relative DCSs measured as a function of the incident energy include statistical errors (0.2%–1.5%) and short-term stability errors (4%–8%). Furthermore, since the relative energy-differential cross sections for NMF are corrected (if needed) according to measured benchmark DCSs for Ar, their overall error could be further increased up to about 15% due to an uncertainty of the reference relative DCS for Ar.

The errors for absolute DCSs, obtained by relative flow technique, include error for reference DCSs for Ar [18] as well as errors of measured signal intensities and flow rates. Due to stable experimental conditions with heating the system and high signal-to-background ratio, the uncertainties of the signal intensities and obtained flow rates are small and therefore the overall error is dominantly defined by the error of reference absolute DCSs for Ar, which we assume to be about 20%. The latter thus defines a minimal uncertainty for our results, while the overall error of the present absolute elastic DCSs for NMF is estimated to be around 25%.

III. CALCULATIONS

Present calculations of molecular cross sections are based on a corrected form of the independent atom method (IAM), known as the screen corrected additivity rule (SCAR) procedure, with an improved quasifree absorption model potential, which includes relativistic and many-body effects, as well as inelastic processes. The same theoretical method has been already used in our recent work on deoxyribose analog molecules (see [10,11]) and pyrimidine base analog [12], where an excellent agreement with experimental results has been obtained in the present angular and energy range, considering the shape of both angular and energy dependence of elastic DCSs, as well as their absolute values.

The SCAR procedure has been described in detail previously [10,26–28]. Briefly, the role of SCAR correction to the standard IAM procedure is reducing the values obtained from the standard additivity rule to account for geometrical overlapping of atomic cross sections. The standard IAM approximation is based on reducing the problem of electron-molecule collisions to collisions with individual atoms by assuming that each atom of the molecule scatters independently and that redistribution of atomic electrons due to the molecular binding is unimportant. At low energies, where atomic cross sections are not small compared to (squared) interatomic distances in the molecule, the IAM approximation fails because the atoms can no longer be considered as independent scatterers and multiple scattering within the molecule is not negligible (note that the energy range for which deviations from the IAM approximation are relevant depends on the molecule). To account for this, screening coefficients are introduced in the present SCAR method, resulting in a corrected cross section of a molecule, at a given incident energy, calculated from the atomic cross sections [10]. In addition, a normalization procedure during the computation of the DCSs has been employed to ensure the consistency of the derived ICSs with the optical theorem [11,12].

The method for calculation of the corresponding atomic cross sections has also been described in detail previously [26,27] and will not be repeated here. Basically, the electron-atom interaction is represented by the approximate *ab initio* optical potential $V_{\rm opt}(r) = V_s(r)+V_e(r)+V_p(r)+i\,V_a(r)$. Here $V_s(r)$ is the static potential calculated by using the charge density deduced from Hartree-Fock atomic wave functions including relativistic corrections, $V_e(r)$ is the exchange potential (to account for the indistinguishability of the incident and target electrons), $V_p(r)$ represents the target polarization potential (accounting for the long-range interactions which depend on the target dipole polarizability), and finally the absorption potential $V_a(r)$ accounting for inelastic processes is

based on the revised quasifree model (see [10,26,27] for more details about the potentials and the theoretical procedure).

IV. RESULTS AND DISCUSSION

The absolute experimentally obtained DCSs for elastic scattering of electrons from the NMF molecule are tabulated in Table I. Relative flow measurements were performed for the incident electron energies of 50, 100, 150, 200, 250, and 300 eV, at several scattering angles (40° and 80° or 90°). Apart from experimental challenges connected with the relative flow method (see Sec. II), the accuracy of the final absolute DCSs also depends on the used referent cross section data set for Ar. According to our knowledge, there are only a few papers that report either independently measured [18,23] or calculated [22] absolute elastic DCSs for Ar in the energy range of interest for the present work. The published results by different authors are not always in perfect agreement. For example, at 100 eV and 40° the elastic e/Ar DCSs reported by Srivastava *et al*. [23] and Nahar and Wadehra [22] appear to be about 12% lower and 50% higher, respectively, than the DCS reported by Williams and Willis [18]. In the present work, the results of Williams and Willis [18] are used because only those are published for the incident electron energies between 20 and 400 eV, thus covering the whole energy range of the present work and allowing to obtain a consistent set of referent DCSs for NMF. The experimentally obtained elastic absolute DCSs for e-NMF scattering are presented in Fig. 2 by circles. The points corresponding to absolute measurements that were used for calibration are presented by stars. The latter fit very well to the relative DCS shape, which is independently obtained. The measured DCSs are compared with theoretical calculations obtained by the SCAR procedure (solid curve in Fig. 2). As already confirmed previously for other molecules [10–12], theoretical and experimental results are in very good agreement, both in shape and absolute values. In the present case for NMF, only a small disagreement appears in the lower angular range (20°–40°). An explanation for this could be a deviation of experimental DCSs, since measurements at small scattering angles are less accurate due to higher background contributions and less reliable volume corrections, especially for low incident energies (e.g., 50 eV) because of larger divergence of the electron beam. However, it should be also noted that SCAR calculations are less accurate at small angles (see [11]). Therefore, as already pointed out in our previous papers, a more detailed study with both an improved experimental setup and theoretical approaches should be performed to accurately resolve forward elastic scattering. It should be also noted that the experimental DCSs are somewhat higher on the absolute scale than theory at 300 eV, in the angular range from 30° to 100°. Good agreement between the experimental and theoretical DSCs, except that it increases the accuracy of both data sets, suggests that SCAR calculations could be used for a reliable estimation of differential cross sections for electron scattering by peptide bond units in the present energy and angular ranges. This is of particular importance for Monte Carlo simulations, such as modeling of radiation damage.

In Fig. 3, one can see that both the experiment and the calculations confirm very similar DCS shapes for NMF and formamide [15]. The angular dependences of the present DCSs for elastic electron-NMF scattering, as well as those for formamide, show a broad minimum at around 90° at lower energies (50 and 100 eV); this disappears at higher energies.

TABLE I. Experimentally obtained differential cross sections for elastic electron scattering from NMF, in units of 10^{-20} m^2 sr^{-1}, as a function of scattering angle and incident electron energy. The absolute errors of relative cross sections (statistical, short-term stability and uncertainty of the effective scattering volume) in the last significant digits are given in parentheses. The errors of the absolute cross sections are estimated to be up to 25%.

	Electron energy (eV)					
Scattering angle (deg)	50	100	150	200	250	300
20	—	4.68(35)	2.36(17)	—	—	1.814(14)
25	—	2.80(21)	1.43(10)	1.1499(91)	0.843(33)	1.0821(98)
30	2.69(55)	1.72(13)	0.889(62)	0.6755(69)	0.62(13)	0.75(15)
35	1.79(37)	1.090(81)	0.564(40)	0.5422(61)	0.458(93)	0.53(11)
40	1.231(54)	0.735(54)	0.446(31)	0.356(71)	0.303(62)	0.315(63)
45	0.922(42)	0.441(94)	0.344(73)	0.240(48)	0.205(42)	0.221(44)
50	0.722(34)	0.341(73)	0.253(54)	0.169(34)	0.148(30)	0.175(35)
55	0.580(28)	0.264(56)	0.178(38)	0.137(28)	0.1274(53)	0.139(28)
60	0.475(24)	0.195(42)	0.145(31)	0.107(22)	0.1070(45)	0.1149(25)
65	0.378(20)	0.152(32)	0.1251(88)	0.098(20)	0.0929(39)	0.093(19)
70	0.323(17)	0.133(28)	0.1053(75)	0.0928(25)	0.0808(35)	0.080(16)
75	0.269(15)	0.130(28)	0.0982(70)	0.0939(24)	0.0730(31)	0.072(14)
80	0.246(14)	0.1244(93)	0.0941(67)	0.0822(22)	0.0689(30)	0.064(13)
85	0.249(14)	0.1180(88)	0.0896(64)	0.0808(23)	0.0581(26)	0.050(10)
90	0.233(14)	0.1119(84)	0.0887(63)	0.0743(22)	0.0506(23)	0.0444(90)
95	0.224(13)	0.1207(90)	0.0874(62)	0.0719(22)	0.0462(21)	0.0399(81)
100	0.227(13)	0.1306(98)	0.0876(62)	0.0658(21)	0.0443(20)	0.0395(80)
105	0.253(14)	0.148(11)	0.0912(65)	0.0655(21)	0.0417(19)	0.0355(72)
110	0.269(15)	0.164(12)	0.0921(65)	0.0610(20)	0.0403(19)	0.0350(13)

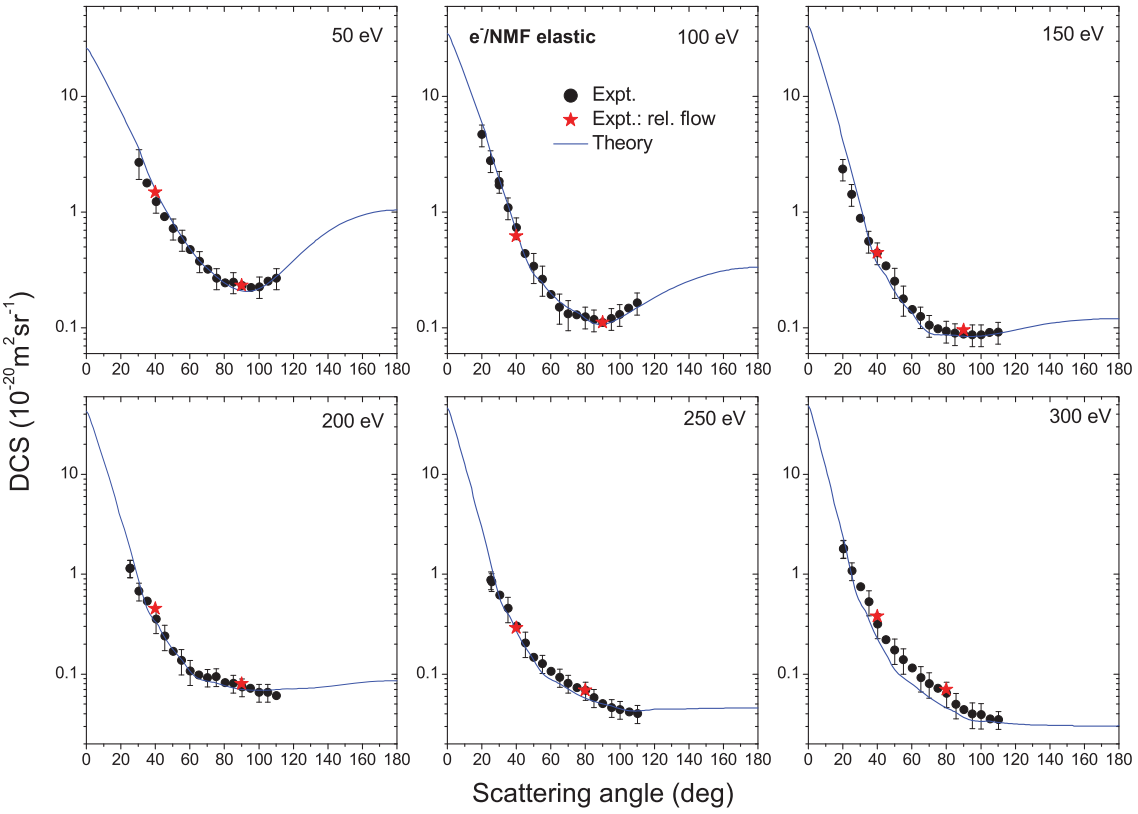

FIG. 2. (Color online) Angular dependence of absolute differential cross sections for elastic electron scattering from *N*-methylformamide at different incident energies. Circles represent the final absolute experimental differential cross sections, stars represent absolute values obtained by relative flow measurements; the calculations are presented by the solid line.

It is also interesting to note that very similar behavior has already been seen in our previous studies of biomolecules representing deoxyribose [10,11] and pyrimidine bases [12]. This suggests a similar distribution of elastically scattered electrons from DNA building blocks, as well as peptide units. Besides the very similar angular dependence of DCSs for NMF and formamide, a small but expected difference on the absolute scale due to the sizes of the molecules (NMF: C_2H_5NO, formamide: CH_3NO) is clearly observable in Fig. 3. Since the difference between the molecules is CH_2 (see Fig. 1), the difference between corresponding absolute DCSs should be similar to absolute DCSs for methane molecule (CH_4) at a given energy, if the building-block approach is valid in this energy range. Indeed, the difference between the present absolute experimental DCSs, (DCS_{NMF}–$DCS_{formamide}$) plotted as a function of the scattering angle, agrees very well, both in shape and on the absolute scale, with the most recently published experimental absolute DCSs for methane [29,30]. Although some deviations can be seen at 45° and 50° for the 100-eV incident energy, the two sets of data are very close considering the experimental errors and a small difference between the absolute cross sections. At the incident energy of 300 eV, the results overlap perfectly. Therefore, the present experimental method is capable of measuring the absolute DCSs with high sensitivity (note, however, that an uncertainty of the absolute position of all DCSs still depends on the referent DCSs for Ar). But more important, the study presented in the insets of Fig. 3 suggests that the building-block approach could be used, at least in the present energy range, for a reliable estimation of DCSs for elastic electron scattering by large macromolecular structures, starting from DCSs of their constituents, which can be accurately obtained.

The dependence of absolute DCSs for elastic electron-NMF scattering on the incident electron energy at a fixed scattering angle of 40° is shown in Fig. 4. Experimental measurements (circles) are normalized on the absolute scale according to DCS values (stars) which have been extracted from the absolute angular-dependent DCSs. Directly measured energy-dependent DCSs at 40° fit very well the points extracted from the absolute angle differential cross sections (biggest disagreement is at 300 eV, around 20%). The calculated DCSs (solid line) for NMF, obtained by the SCAR procedure, have been presented in the energy range 40–300 eV. The SCAR method gives slightly lower results on the absolute scale (except at 50 eV), but generally confirms absolute values and the behavior of the energy-dependent cross sections. Results for the formamide molecule are also presented in Fig. 4, showing very similar behavior. Absolute measured points for formamide (pentagons) are extracted from angular-dependent DCSs, at 100, 150, and 300 eV [15]. Experimental points for formamide are also higher on the absolute scale than the calculated one, but within absolute error (25%). As expected according to molecular sizes, absolute DCS for NMF is higher on the absolute scale than for formamide. However, it should be

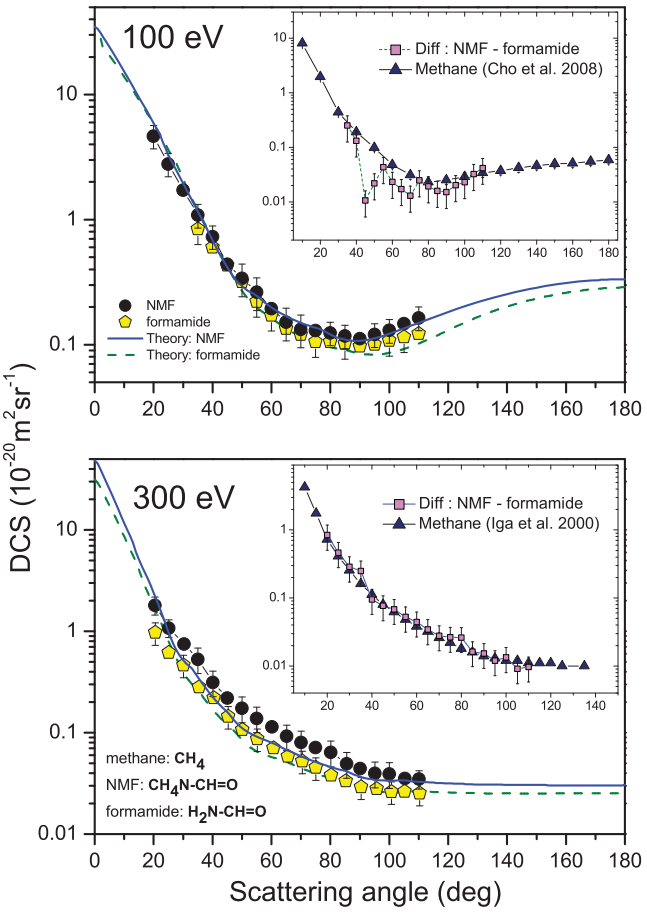

FIG. 3. (Color online) Angular dependence of absolute differential cross sections for elastic electron scattering from formamide and *N*-methylformamide (NMF) at the incident energies of 100 and 300 eV. The experimental results are presented by circles (NMF) and pentagons (formamide, [15]). The theoretical results are presented by solid line (NMF) and dashed line (formamide, [15]). The inset shows a comparison of the difference between absolute DCSs for NMF and formamide (squares, DCS_{NMF}–$DCS_{formamide}$) with the most recent experimental results for methane (triangles, CH_4) published by Cho *et al.* [29] (100 eV) and Iga *et al.* [30] (300 eV).

noted that the latter difference between calculated differential cross sections at 40° slightly increases with increasing the incident electron energy (overall about 10% from 50 to 300 eV).

The present calculated integral cross sections for electron scattering from both NMF and formamide are given in Fig. 5 and tabulated in the Supplemental Material [31]. Integral elastic cross sections are the results of the integration of the molecular differential elastic cross sections for all the scattering angles (from 0° to 180°). Using our normalization procedure these results are equal to the sum of the atomic integral elastic cross sections, in agreement with the optical theorem (thus avoiding the contradiction shown for other IAM calculations). The electronically inelastic integral cross sections are determined by applying the SCAR procedure to the atomic integral inelastic cross sections derived from our absorption potential. We add "electronically" just to indicate that molecular vibrations or rotations are not included in

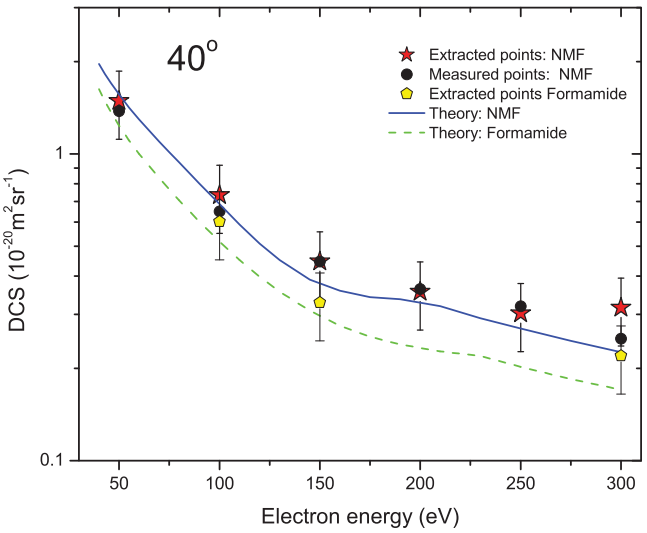

FIG. 4. (Color online) Energy dependence of absolute differential cross sections for elastic electron scattering from *N*-methylformamide (NMF) and formamide at the scattering angle of 40°. (Stars) experimental points for NMF extracted from the present tabulated absolute DCSs; (circles) direct independent measurement for NMF as a function of the incident energy, normalized at 150 eV; (pentagons) experimental points for formamide extracted from published tabulated absolute DCSs [15]; (solid line) theory for NMF; (dashed line) theory for formamide.

our calculation. The integral cross sections (ICSs) for elastic scattering by NMF and formamide have very similar behavior, decreasing monotonically in the used energy range. From 10 to 1000 eV of the incident electron energy, they drop for about one order of magnitude. The ICS for formamide is about 25% lower at the absolute scale in comparison with NMF.

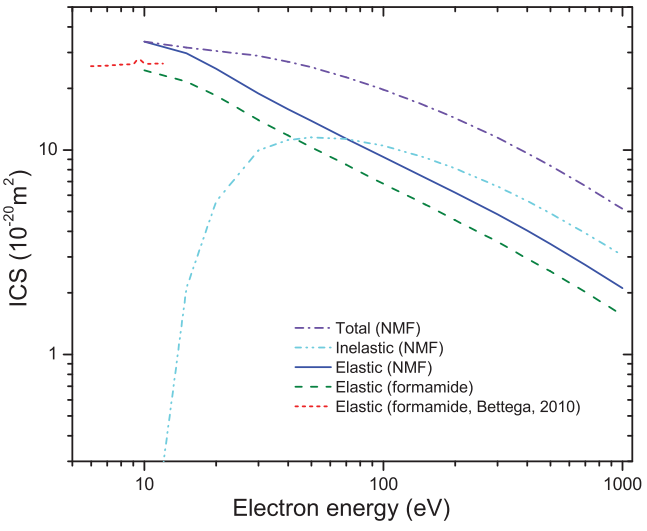

FIG. 5. (Color online) Calculated total cross section (dash-dot), integral electronically inelastic cross section (dash-dot-dot), and integral elastic cross section (solid line) for electron scattering from NMF molecule. The integral elastic cross section for electron scattering from formamide molecule calculated by the present method (long dash) and previously calculated in the static-exchange-polarization approximation by Bettega [16] (short dash) are presented as well.

According to our knowledge, there are no published ICSs for NMF. On the other hand, Betega [16] has very recently reported integral and momentum transfer cross sections for elastic scattering of low-energy electrons (1–12 eV) by formamide, calculated by employing the Schwinger multichannel method with pseudopotentials in the static-exchange and in the static-exchange-polarization approximations. The integral cross section calculated in the static-exchange-polarization approximation is compared with the present results in Fig. 5 (short-dashed line). Considering absolute values, this result agrees very well with the present calculation (dashed line). A discrepancy can be seen in the region from about 9 to 12 eV, where the previous ICS remains practically constant while the present results show a decrease. It should be noted that the present calculations based on the independent atom model are basically limited to higher energies, even including improved SCAR procedure accounting for the overlap of the cross sections (see Sec. III and references therein for more details). Furthermore, the used SCAR method ignores the rotational and vibrational excitations and considers only those inelastic processes arising from electronic excitation. Although this restriction is not significant in general for the relatively high energies (as used in the present experimental work), in the case of molecules with a relatively high permanent dipole moment, rotational excitation may become more important, especially at lower incident energies [11,28]. Note that the dipole moment for NMF has been reported to be about 3.86*D* [32]. Still, it is important to point out that the ICSs for these molecular targets can be rather accurately reproduced by the present low-cost calculations, even down to about 10 eV.

V. CONCLUSION

The elastic scattering of electrons from the *N*-methylformamide (NMF) molecule has been investigated, both experimentally and theoretically. The experimental absolute DCSs for elastic electron scattering are tabulated for incident electron energies from 50 to 300 eV, in the overall angular region from 30° to 110° (from 20° at 300 eV). The measurements of the relative DCSs were performed as a function of both the scattering angle and the incident energy, using a cross-beam technique. The relative flow measurements, with Ar as the referent gas, provided absolute experimental points which were used to normalize the relative DCSs. The calculations are based on a corrected form of the independent atom method, known as a screen corrected additivity rule procedure. The agreement between the measurements and calculations is very good, regarding both the shape of the DCSs and their absolute values (in the overlapping angular range). The calculated integral cross sections are also presented in the range from 10 to 1000 eV, both for NMF and formamide.

The elastic DCSs for *N*-methylformamide and formamide molecule [15] appear to be very similar in shape, suggesting thus that a substitution of the H atom in formamide with the CH_3 group does not significantly affect the elastic electron scattering processes in this energy range. The DCSs for NMF and formamide are also similar on the absolute scale; however, the measured difference is consistent with the molecular sizes, thus suggesting that the building-block approach is valid in this energy range. Finally, it is interesting to note that both the absolute cross sections and angular distribution of elastically scattered electrons from peptide bond units are similar to the molecules' analogs to DNA building blocks.

The present results contribute to fundamental understanding of electron interaction with biomolecules in the medium incident energy range. The tabulated absolute cross sections for NMF molecule can be used as starting parameters for energy deposition modeling in biologically relevant media.

ACKNOWLEDGMENTS

The work was supported by the Ministry of Education and Science of Republic of Serbia (Project No. 171020) and Spanish Ministerio de Ciencia e Innovación Project No. FIS2009-10245, and motivated by the COST Action MP1002 (Nano-IBCT). We are also grateful to Dr. A. Giuliani from SOLEIL for discussion that initiated this work.

[1] S. Leach, H. W. Jochims, and H. Baumgärtel, J. Phys. Chem. A **114**, 4847 (2010).
[2] J. M. Hollis, F. J. Lovas, A. Remijan, P. R. Jewell, V. Ilushin, and I. Kleiner, Astrophys. J. **L25**, 643 (2006).
[3] A. Lafosse, M. Bertin, A. Domaracka, D. Pliszka, E. Illenberger, and R. Azria, Phys. Chem. Chem. Phys. **8**, 5564 (2006).
[4] K. Graupner, T. L. Merrigan, T. A. Field, T. G. A. Youngs, and P. C. Marr, New J. Phys. **8**, 117 (2006).
[5] B. Boudaiffa, P. Cloutier, D. Hunting, M. A. Huels, and L. Sanche, Science **287**, 1658 (2000).
[6] B. D. Michael and P. O. Neil, Science **287**, 1603 (2000).
[7] A. V. Solov'yov, E. Surdutovich, E. Scifoni, I. Mishustin, and W. Greiner, Phys. Rev. E **79**, 011909 (2009).
[8] COST Action MP1002, Nanoscale insights into Ion Beam Cancer Therapy (Nano-IBCT); [http://fias.uni-frankfurt.de/nano-ibct/overview/].
[9] E. Scifoni, E. Surdutovich, and A. V. Solov'yov, Phys. Rev. E **81**, 021903 (2010).
[10] A. R. Milosavljević, F. Blanco, D. Šević, G. García, and B. P. Marinković, Eur. Phys. J. D **40**, 107 (2006).
[11] A. R. Milosavljević, F. Blanco, J. B. Maljković, D. Šević, G. Garsia, and B. P. Marinković, New J. Phys. **10**, 103005 (2008).
[12] J. B. Maljković, A. R. Milosavljević, F. Blanco, D. Šević, G. García, and B. P. Marinković, Phys. Rev. A **79**, 052706 (2009).
[13] Y. Kawashima, T. Usami, N. Ohashi, R. D. Suenram, J. T. Hougen, and E. Hirota, Acc. Chem. Res. **39**, 216 (2006).
[14] M. Iwakawat, P. J. Tofilon, N. Hunter, L. C. Stephens, and L. Milas, Clin. Exp. Metastasis **5**, 289 (1987).
[15] J. B. Maljković, F. Blanco, G. García, B. P. Marinković, and A. R. Milosavljević, Nucl. Instrum. Methods Phys. Res., Sect. B **279**, 124 (2012).
[16] M. H. F. Bettega, Phys. Rev. A **81**, 062717 (2010).

[17] A. R. Milosavljević, S. Mandžukov, D. Ševic, I. Čadež, and B. P. Marinković, J. Phys. B **39**, 609 (2006).
[18] J. F. Williams and B. A. Willis, J. Phys. B **8**, 1670 (1975).
[19] J. C. Nickel, C. Mott, I. Kanik, and D. C. McCollum, J. Phys. B **21**, 1867 (1988).
[20] J. C. Nickel, P. V. Zetner, G. Shen, and S. Trajmar, J. Phys. E **22**, 730 (1989).
[21] M. A. Khakoo, K. Keuane, C. Campbell, N. Guzman, and K. Hazlett, J. Phys. B **40**, 3601 (2007).
[22] S. N. Nahar and J. M. Wadehra, Phys. Rev. A **35**, 2051 (1987); **43**, 1275 (1991).
[23] S. K. Srivastava, H. Tanaka, A. Chutjian, and S. Trajmar, Phys. Rev. A **23**, 2156 (1981).
[24] H. Silva, J. Muse, M. C. A. Lopes, and M. A. Khakoo, Phys. Rev. Lett. **101**, 033201 (2008).
[25] M. G. P. Homem, I. Iga, R. T. Sugohara, I. P. Sanches, and M. T. Lee, Rev. Sci. Instrum. **82**, 013109 (2011).
[26] F. Blanco and G. García, Phys. Lett. A **317**, 458 (2003).
[27] F. Blanco and G. García, Phys. Lett. A **330**, 230 (2004).
[28] A. Muñoz, J. C. Oller, F. Blanco, J. D. Gorfinkiel, P. Limão-Vieira, and G. Garcia, Phys. Rev. A **76**, 052707 (2007).
[29] H. Cho, Y. S. Park, E. A. y. Castro, G. L. C. de Souza, I. Iga, L. E. Machado, L. M. Brescansin, and M.-T. Lee, J. Phys. B **41**, 045203 (2008).
[30] I. Iga, M.-T. Lee, M. G. P. Homem, L. E. Machado, and L. M. Brescansin, Phys. Rev. A **61**, 022708 (2000).
[31] See Supplemental Material at http://link.aps.org/supplemental/10.1103/PhysRevA.85.042723 for tabulated theoretical integral elastic, integral inelastic, and total cross sections for electron scattering from *N*-methylformamide and formamide.
[32] G. G. Almeida and J. M. M. Cordeiro, J. Braz. Chem. Soc. **22**, 2178 (2011).